



## Statistical evaluation of the effect of hygrothermal aging on the interlaminar shear of GFRP

Dmitrii S. Lobanov, Andrey S. Yankin, Nataliya I. Berdnikova

Perm National Research Polytechnic University, Russia

*cem.lobanov@gmail.com, http://orcid.org/0000-0003-1948-436X*

*yas.cem@yandex.ru, https://orcid.org/0000-0002-0895-4912*

*natalya.berdnikova2017@yandex.ru*

**ABSTRACT.** The studies of patterns of changes in properties, accumulation of damages and failure of structural composites after hygrothermal aging represent a relevant and important area. The paper presents the results of mechanical tests for interlaminar shear of specimens of structural glass/epoxy composite electrical use before and after preliminary hygrothermal aging in operating environments (process water, sea water, machine oil) of various duration (15, 30 and 45 days) and various temperatures (22, 60 and 90 °C). The test results were used to statistically evaluate the significance of non-monotonous changes in strength in the case of interlaminar shear after preliminary hygrothermal aging relative to the nominal material using ANCOVA and regression analysis. Such techniques indicated that sea and process water solutions negatively affected the interlaminar shear strength, but their influences were slightly different and strongly depended on the interaction effect between exposure time and solution temperature. Thus, the maximum difference is around 15 % and 12 % after 45 days inside process and sea water respectively at 90 °C. On the contrary, the impact of machine oil led to an increase in strength, but the effect is weaker compared to water solutions (about 6 %).

**KEYWORDS.** Hygrothermal aging; Aggressive operating media (environments, solutions); Interlaminar shear strength; GFRP; ANCOVA; Multiple linear regression.



**Citation:** LobanovD, S., Yankin A.S., Berdnikova N.I. Statistical evaluation of the effect of hygrothermal aging on the interlaminar shear of GFRP, *Frattura ed Integrità Strutturale*, 60 (2022) 146-157.

**Received:** 24.12.2021

**Accepted:** 21.01.2022

**Online first:** 27.01.2022

**Published:** 01.04.2022

**Copyright:** © 2022 This is an open access article under the terms of the CC-BY 4.0, which permits unrestricted use, distribution, and reproduction in any medium, provided the original author and source are credited.

## INTRODUCTION

When composite materials are implemented, special importance is given to the analysis of failure conditions and durability of products. A relevant task is to study and analyze the effects of high and low (operating) temperatures on mechanical properties and failure mechanisms of reinforcing and composite materials as well



as the definition of temperature dependencies of elastic and strength properties of fiber composites used in critical structures. Experimental data concerning the effects of operating and climatic temperatures on mechanical properties of various classes of polymeric composite materials are represented in [1-4].

To predict the operating life of structures made of polymeric composites, it becomes relevant to study the matters related to the aging of polymeric composite materials. The aging of polymeric composites is a ubiquitous issue that leads to impaired mechanical properties, the reduced design life of the structure and potential early failure. The issue of the aging of polymeric composites in the aqueous environment is studied in [5-8]. Most structures of polymeric composites are subject to atmospheric factors during operation (temperature, humidity, solar radiation, cyclic changes in temperature, tropical and sea climate, etc.) that affect their physical, chemical and mechanical properties.

It becomes important to study the issues of hygrothermal aging of polymeric composites since it is possible to accelerate aging processes during temperature rise. The studies of trends in changes of physical and mechanical properties of polymeric composites based on glass, carbon and basalt fiber and epoxy, acrylic and nylon thermal-plastic binders in case of hygrothermal aging in various media (distilled water, sea water, machine oil, alkali solutions, etc.) are found in [8-19]. Primary attention in these papers is paid to the studies of degradation in microstructure and diffusion of a liquid medium. The papers fail to consider or pay little attention to statistical evaluation of results and further comparative analysis of effects of hygrothermal aging on the changes in mechanical characteristics and failure mechanisms of structural composites.

Representing experimental data should be easily interpreted and understood, therefore statistical methods are extremely important for that. Obviously, test data may have not only quantitative but also categorical variables (for instance, aggressive environments). In this case, ANOVA (Analysis of Variance), ANCOVA (analysis of covariance), regression, and other related procedures might be applied [20, 21]. For example, such methods were utilized to examine the effects of various reinforcement types on properties of wood polymer composites before and after aging [22], the effect of hydrothermal aging (thermal cycles from -28 °C to 85 °C in air, distilled water and salt water) on the mechanical resistance of single lap bonded CFRP joints [23], sample orientation and geometry on the mechanical response of additively manufactured commercially pure titanium [24], different implant abutment designs on fracture resistance and bending moment [25], different storage media and exposure time on the hardness of CAD/CAM composite blocks [26]. Furthermore, those techniques are widely used to indicate the most contributing input parameters and select the optimal combination of them to obtain the required results [27-31]. In the current study, a statistical approach using ANCOVA multiple linear regression analysis was used to investigate the effects of 3 different aggressive environments, temperature, exposure time, and their interactions on mechanical properties of structural GFRP, to assess which factors are statistically significant and to develop a prediction model.

## MATERIAL AND EXPERIMENTAL PROCEDURE

The material used in the study is the general-purpose construction fiberglass laminate STEF (ST - fiberglass, EF - epoxy-phenol-formaldehyde or epoxy binder). It is laminated reinforced fiberglass obtained by hot pressing of fiberglass cloth impregnated with a thermoreactive compound based on combined epoxide and phenol-formaldehyde resins. Experimental study of structural fiberglass/epoxy "STEF" specimens after hygrothermal aging in different liquids (process water, sea water, machine oil) at 22, 60 and 90°C for 15, 30 and 45 days is carried out (Table 1). Mechanical tests for interlaminar shear under static conditions were carried out using the short beam method on the basis of the shared research facilities "Center of Experimental Mechanics" in Perm National Research Polytechnic University (PNRPU). Mechanical tests were conducted according to recommendations of ASTM D2344 using an Instron 5965 electromechnical testing system. The loading rate was 1 mm / min. The dimensions of the specimens were 24x8x4 mm. The distance between the supports was 20mm. As a result of the tests, the interlaminar shear strength was determined by the formula (1):

$$F^{sbs} = 0.75 \cdot \frac{P_m}{b \cdot h} \quad (1)$$



where  $F_{sbs}$  is short-beam strength or interlaminar shear strength, (MPa);  $P_m$  is maximum load observed during the test, (N);  $b$  is measured specimen width, (mm), and  $h$  is measured specimen thickness, (mm).

The procedure of specimen preparation and preliminary hygrothermal aging was as follows. Cut-out specimens were divided into groups, marked, weighed and put into baths with prepared liquid media: sea water (salinity coefficient of 30 %), process water and machine oil (synthetic oil for automobile engines). Some containers remained in laboratory conditions, while others were put to chambers at a constant temperature of 60 and 90 °C for 45 days. During exposure, evaporation was visually monitored on a daily basis; if necessary, the medium was topped up with a liquid preliminary heated to the required temperature. The specimens were extracted after 15, 30 and 45 days of exposure, wiped with a cotton cloth and left for a day in the open air at laboratory conditions, then were weighed. Before testing, the microstructure of the specimen surface was recorded after aging in a non-loaded state. After that, fiberglass specimens were tested for interlaminar shear (short beam method) with further study of the microstructure and analysis of failure mechanisms.

Liquids	Temperature, °C	Without aging / control samples		Exposure time, days		
		15	30	45		
Machine Oil	22					
	60					
	90					
Sea Water	22					
	60	3 specimens	3 specimens on “point”	3 specimens on “point”	3 specimens on “point”	
	90					
Process Water	22					
	60					
	90					

Table 1: Program of mechanical testing after different modes of pre-exposure hygrothermal aging

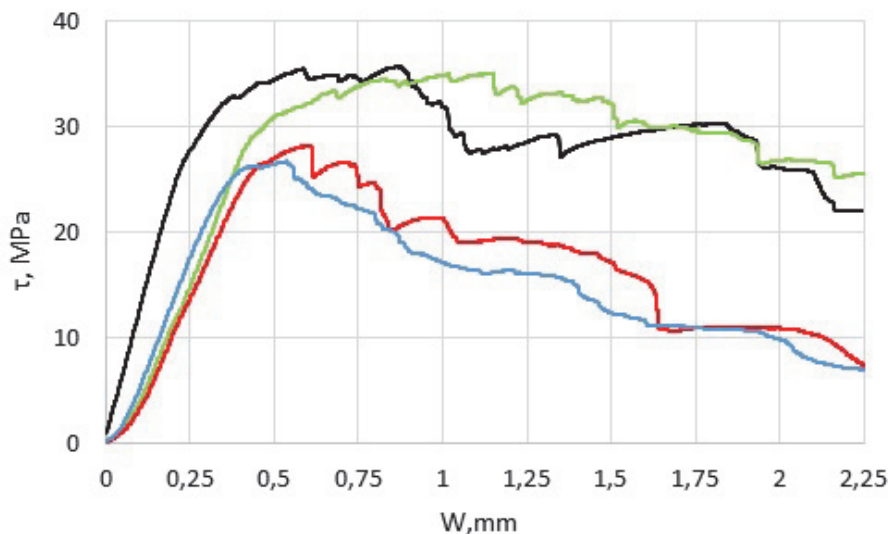


Figure 1: Typical loading diagram of interlaminar shear test for fiberglass/epoxy “STEF” specimens: without aging (black line), after aging in machine oil (green line), sea water (red line); process water (blue line) at temperature of 90 °C and time of 45 days.

## RESULT AND DISCUSSIONS

Tests were performed at the Center of Experimental Mechanic in order to evaluate the degradation of composite material properties under aggressive solutions. For reference, Fig. 1 shows characteristic diagrams of fiberglass specimen loading without hygrothermal aging and after hygrothermal aging of the highest intensity (45 days, 90 °C) for each of the studied media. These deformation diagrams show that there is reduced bending rigidity after aging for all specimens (the incline angle of the diagram linear section is reduced). Similar results of the studies are found in [19, 32, 33] for other types of static tests.

Fig. 2 gives an image of the surface microstructure of fiberglass specimens before and after interlaminar shear for a specimen without aging (Fig. 2a) and after hygrothermal aging at exposure conditions of 45 days / 90 °C in machine oil (Fig. 2b), sea water (Fig. 2c) and process water (Fig. 2d). For all tested specimens without aging and after aging in machine oil, primary failure starts on the elongated surface (Fig. 2a, 2b yellow ellipse) with further interlaminar shear of lower and middle layers. Inter-layer fractures are local in the specimen center under the loading pin (Fig. 2a, 2b red ellipse). For specimens after aging in sea water and process water (Fig. 2c,d), a good failure pattern is observed. Specimens fail in a brittle manner, and there is joint failure due to elongation and interlaminar shear. There are large main cracks (Fig. 2c, 2d white ellipse) between middle layers, which come from specimen edges. The material is crushed at the place where pin loading is applied, with further local lamination (Fig. 2c, 2d red ellipse).

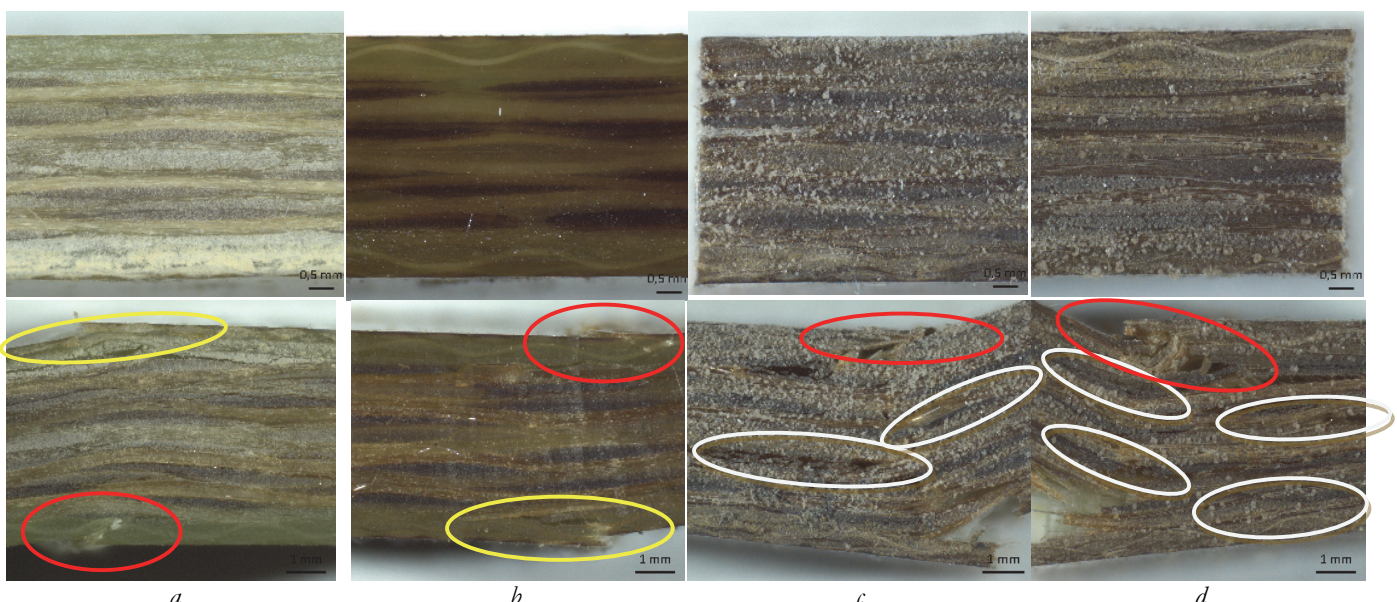


Figure 2: Surface structure of fiberglass specimens before and after interlaminar shear testing: specimen without aging (a); specimen after aging in machine oil during 45 days at 90 °C (b); specimen after aging in sea water during 45 days at 90 °C (c); specimen after aging in process water during 45 days at 90 °C (d).

As a result, weight gain and interlaminar shear strength values for all conditions were determined (Table 2-3). In order to see the data distribution, skewness, and outliers, the box plot chart (Fig. 3) was plotted. From Fig. 3a one can see that strength values are not too skewed and there are no outliers, therefore we can accept the whole dataset. Oppositely, Fig. 3b illustrates 5 outliers for weight gain values, so we should remove them for further study.

Table 2 lists average values of the interlaminar shear strength of all specimens tested, calculated by Eq. (1). It is possible to observe that, the results have changed after immersion into solutions over the exposure time. The analysis of the results from Table 2 indicates that process water promotes lower strength than the sea water relative to the control samples. This effect depends on the exposure time and solution temperature: the higher temperature and time, the lower strength. On the contrary, universal machine oil makes strength values slightly bigger. Similarly, this effect is dependant on solution temperature.

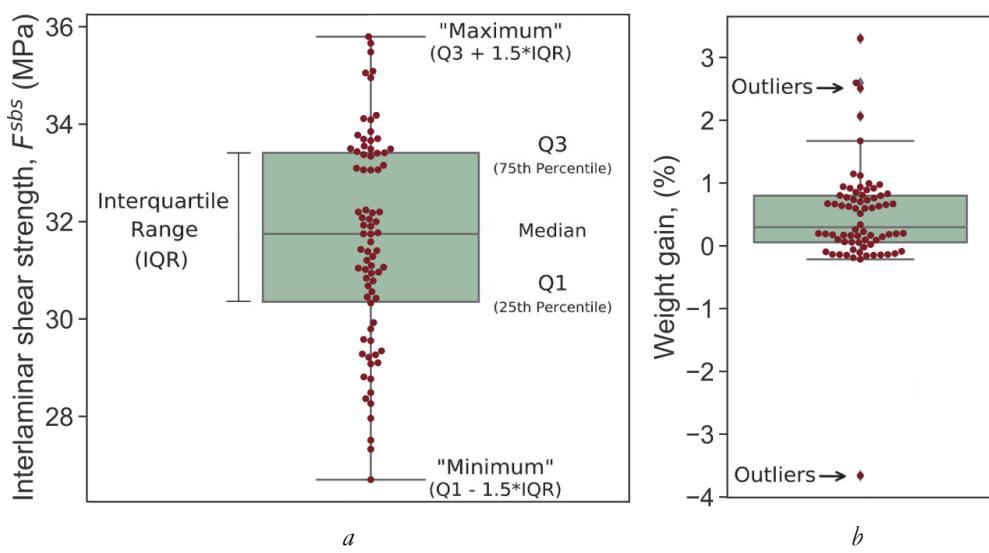


Figure 3: Box plot diagrams of interlaminar shear strength (a) and weight gain (b) values

Environment/ Temperature, °C	Aver. interlaminar shear strength, (MPa)		
	15 days	30 days	45 days
<b>Control samples (without aging)</b>	31.7	-	-
<b>Machine oil</b>			
22	-	32.4	33.1
60	-	33.7	32.2
90	-	34.3	33.2
<b>Sea water</b>			
22	34.0	33.7	33.2
60	33.7	32.1	31.2
90	30.	29.1	28.2
<b>Process water</b>			
22	33.0	30.9	33.4
60	30.9	29.6	30.2
90	29.1	29.8	27.2

Table 2: Effect of the solutions, their temperature, and exposure time on the interlaminar shear strength in terms of average values

Table 3 demonstrates the average weight gain values for all operating environments. It is clearly shown a negligible weight change in terms of the machine oil solution. As we can see, sometimes specimens even lose weight after immersion tests into the machine oil. However, different behavior is observed for the sea and process water solutions. In this case, an increase can be observed compared to the dry specimens.



Environment	Temperature, °C	Weight gain (%)		
		15 days	30 days	45 days
Machine oil	22	0.10	0.02	-
	60	0.06	-0.09	-0.10
	90	-0.14	-0.15	0.15
Sea water	22	0.18	0.33	-
	60	0.67	0.79	1.02
	90	0.81	0.77	0.92
Process water	22	0.19	0.18	-
	60	1.67	0.60	0.66
	90	0.65	0.34	1.06

Table 3: Effect of the solutions, their temperature, and exposure time on the weight gain in terms of average values.

## ANCOVA AND REGRESSION ANALYSIS

### Interlaminar shear strength

In this research study, ANCOVA was used for a multiple regression analysis in which there are at least one quantitative and one categorical variables [20]. And by doing this, the categorical variable with 3 kinds of solutions was re-coded as 2 new columns with 0 and 1. The variables were coded 0 for any case that did not match the variable name and 1 for any case that did match the variable name. The whole procedure was carried out by Python software (More information about the code you can find here: <https://github.com/yanicen1/strength-ANCOVA-regression>).

This analysis was applied to examine whether there are differences and interactions between the different solutions, their temperature, and exposure time, as well as to predict the interlaminar shear strength under various conditions. In doing so, two models were developed (Fig. 4 and Tables 4-5). The first one is the additive model, i.e. it does not take into account any interaction effects. The second model adds the interactions to produce the interaction ANCOVA model. By doing this, it is evident that aggressive media, as well as its temperature, do not affect the results at an exposure time of 0 days. Consequently, these input variables can be considered insignificant and removed from the interaction model. Thus, 'Pr. water', 'Sea water', 'Temp', 'Pr. Water × Temp', and 'Sea water × Temp' variables were not taken into account in order to avoid high multicollinearity.

The additive and interaction models explain 34 % and 64 % of the variability in test scores respectively (adjusted R<sup>2</sup> are 0.338 and 0.642), and the standard error of estimate (1.52 and 1.12) represents how far data fall from the regression predictions. Hereby, it suggests that the second model is the better one (Table 4). In addition, from Table 4 one can see that the test has F statistic 'F-value' of 31.24 and 13.92 with p-values of less than 0.001 for additive and interaction models respectively. Accordingly, it shows the necessity of these models over an intercept-only model that predicts the average output for all the data.

Model	R <sup>2</sup>	Adjusted R <sup>2</sup>	Std. Error of Estimate	F-value	p-value
Add. mod.	0.365	0.338	1.52	13.92	< 0.001***
Full mod.	0.664	0.642	1.12	31.24	< 0.001***

Significance levels: \*\*\*p-val. ≤ 0.001 (significant), \*\*p-val. ≤ 0.01 (very significant), \*p-val. ≤ 0.05 (highly significant).

Table 4: Model summary results for interlaminar shear strength.

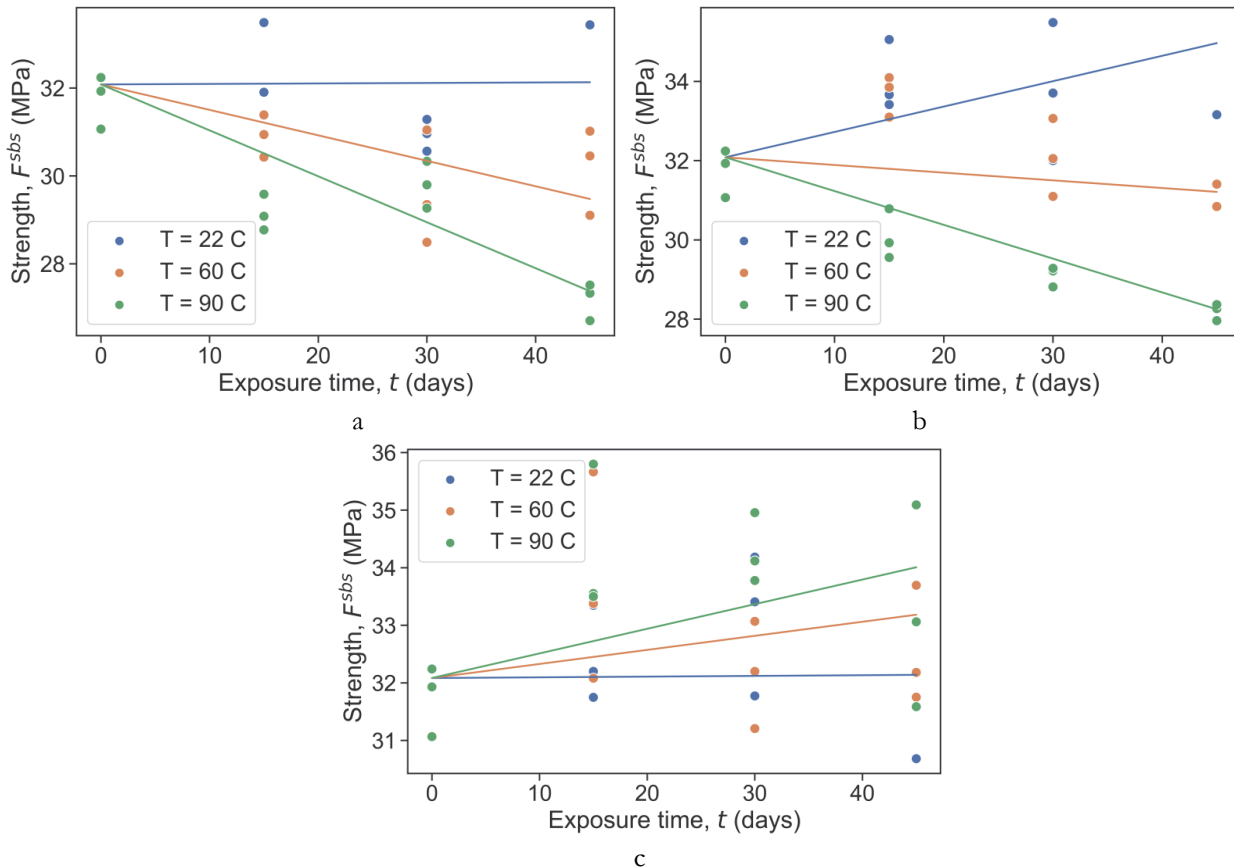


Figure 4: Relationship between interlaminar shear strength and exposure time for the composite exposed to process water (a), sea water (b), and machine oil (c) solutions at different temperatures

	Model	Coefficient	Std. Error	t-value	p-value	Confidence Interval	
						[0.025	0.975]
1	Const.	34.49	0.45	76.75	< 0.001***	33.60	35.39
	Pr. water	-2.125	0.369	-5.753	< 0.001***	-2.858	-1.392
	Sea water	-1.129	0.369	-3.057	0.003**	-1.862	-0.396
	Temp.	-0.0223	0.006	-4.003	< 0.001***	-0.0334	-0.0112
	Time	-0.0195	0.009	-2.092	0.039*	-0.0379	-0.0010
2	Const.	32.08	0.18	176.14	< 0.001***	31.72	32.45
	Time	-0.0122	0.0200	-0.609	0.544	-0.0520	0.0276
	Temp. $\times$ Time	0.00061	0.00028	2.182	0.032*	0.00006	0.00117
	Pr. water $\times$ Temp. $\times$ Time	-0.0022	0.0004	-5.478	< 0.001***	-0.0030	-0.0014
	Pr. water $\times$ Time	0.0475	0.0270	1.762	0.081	-0.0060	0.1011
	Sea water $\times$ Temp. $\times$ Time	-0.0028	0.0004	-7.096	< 0.001***	-0.0036	-0.0020
	Sea water $\times$ Time	0.1245	0.0270	4.615	< 0.001***	0.0710	0.1780

Significance levels: \*\*\*p-val.  $\leq 0.001$  (significant), \*\*p-val.  $\leq 0.01$  (very significant), \*p-val.  $\leq 0.05$  (highly significant).

Table 5: Multiple linear regression results for interlaminar shear strength.

Reviewing the regression results of the effect of the solutions on the interlaminar shear strength in Fig. 4 and Tables 5, model 2 can be represented as

$$F_{shs} = 30.08 - 0.0122 \times \text{Time} + 0.00061 \times \text{Temp.} \times \text{Time} - \\ - 0.0022 \times \text{Pr.Wat.} \times \text{Temp.} \times \text{Time} + 0.0475 \times \text{Pr.Wat.} \times \text{Time} - \\ - 0.0028 \times \text{SeaWat.} \times \text{Temp.} \times \text{Time} + 0.1245 \times \text{SeaWat.} \times \text{Time}$$

The simplified model equations are shown here

Machine oil:  $F_{shs} = 30.08 - 0.0122 \times \text{Time} + 0.00061 \times \text{Temp.} \times \text{Time}$

Pr. water:  $F_{shs} = 30.08 + (-0.0122 + 0.0451) \times \text{Time} + (0.00061 - 0.0022) \times \text{Temp.} \times \text{Time}$

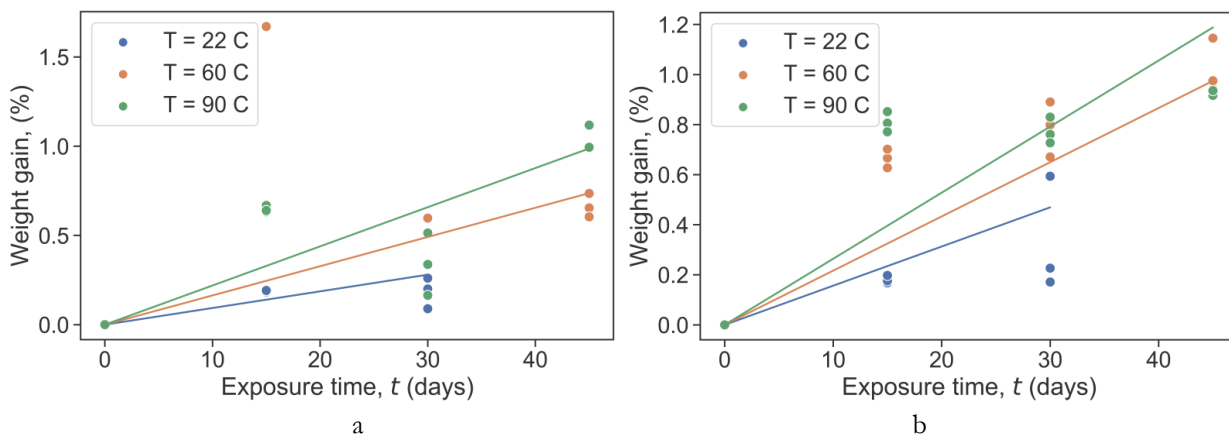
Sea water:  $F_{shs} = 30.08 + (-0.0122 + 0.1245) \times \text{Time} + (0.00061 - 0.0028) \times \text{Temp.} \times \text{Time}$

From the equations, we see that 30.08 (with a 95 % confidence interval from 31.72 to 32.45 MPa) is the mean value of the interlaminar shear strength of the material after immersion tests into the machine oil, sea, and process water solutions over the exposure time of 0 days at any temperature. Also, we can say that this value of 30.08 MPa is statistically different from zero ( $t$ -value = 176.14,  $p$ -value < 0.001). Similarly, the slope of  $F_{shs}$  vs. Time is -0.0122 for machine oil, (-0.0122 + 0.1245) for sea water, and (-0.0122 + 0.0451) for process water respectively. There is a statistically significant effect of exposure time on the interlaminar shear strength only for sea water (the slope  $F_{shs}$  vs. Time of 0.1245,  $t$ -value = 4.615,  $p$ -value < 0.001), which means the mean strength increases by 1.25 MPa for every 10 days inside the saline solution.

In addition, the slope of  $F_{shs}$  vs. Temp.  $\times$  Time (the interaction between temperature and time) for machine oil can be seen to be 0.00061, (0.00061 - 0.0028) for sea water, and (0.00061 - 0.0022) for process water. Again, follow-up linear regression analysis in the form of a  $t$ -test indicates that the interactions for machine oil ( $t$ -value = 2.182,  $p$ -value = 0.032), sea ( $t$ -value = -7.096,  $p$ -value < 0.001) and process water solutions ( $t$ -value = -5.478,  $p$ -value < 0.001) are statistically significant. This result means that for a 1000 unit increase in product 'Temp.  $\times$  Time' is 0.6 MPa increase as well as -2.2 and -1.6 MPa decrease in strength for oil, sea and process water respectively.

## WEIGHT GAIN

A similar analysis was used to study the effects of the operating environments on weight gain (Fig. 5 and Tables 6-7). By doing this, it is clear that weight gain is equal to 0 at an exposure time of 0 days. Therefore, the 'Const' variable was removed from the models. From Table 6 it is apparent that both models are better than an intercept-only model that predicts the average output for the whole dataset ( $F$ -value = 43.48,  $p$ -value < 0.001 and  $F$ -value = 78.64,  $p$ -value < 0.001 for additive and interaction models respectively). Also, the additive and interaction models explain 54 % and 76 % of the variability in test scores respectively (adjusted  $R^2$  are 0.541 and 0.764). The standard errors of estimate are equal to 0.27 and 0.19 and represent how far data fall from the regression predictions. Thus, one can conclude that the interaction model is the better than additive one.



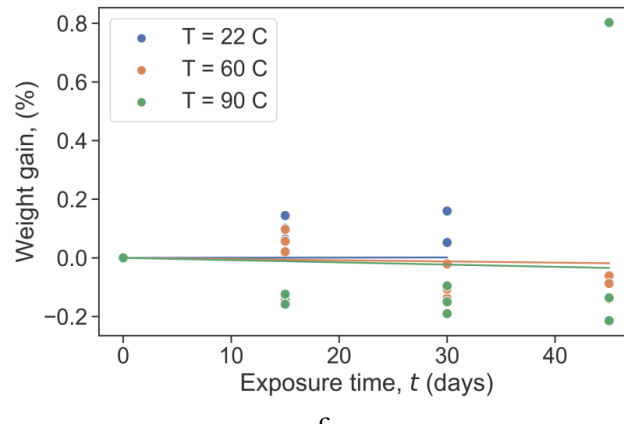


Figure 5: Relationship between weight gain and exposure time for the composite exposed to process water (a), sea water (b), and machine oil (c) solutions at different temperatures

Model	R <sup>2</sup>	Adjusted R <sup>2</sup>	Std. Error of Estimate	F-value	p-value
Add. mod.	0.554	0.541	0.27	43.48	< 0.001***
Full mod.	0.774	0.764	0.19	78.64	< 0.001***

Significance levels: \*\*\*p-val.  $\leq 0.001$  (significant), \*\*p-val.  $\leq 0.01$  (very significant), \*p-val.  $\leq 0.05$  (highly significant).

Table 6: Model summary results for weight gain

	Model	Coefficient	Std. Error	t-value	p-value	Confidence Interval	
						[0.025	0.975]
1	Pr. water	0.167	0.051	3.286	0.001***	0.066	0.267
	Sea water	0.245	0.049	5.019	< 0.001***	0.149	0.342
	Temp.	-0.0010	0.0006	-1.882	0.062	-0.0021	0.0001
	Time	0.0108	0.0014	7.930	< 0.001***	0.0081	0.0135
2	Time	0.0003	0.0039	0.080	0.937	-0.0074	0.0081
	Temp.×Time	-1.2×10 <sup>-5</sup>	5.5×10 <sup>-5</sup>	-0.216	0.829	-0.00012	9.7×10 <sup>-5</sup>
	Pr. water×Temp.×Time	0.00020	8.0×10 <sup>-5</sup>	2.461	0.015*	0.00004	0.00036
	Pr. water×Time	0.0049	0.0056	0.877	0.382	-0.0062	0.0161
	Sea water×Temp.×Time	0.00017	7.8×10 <sup>-5</sup>	2.180	0.031*	0.00002	0.00032
	Sea water×Time	0.0119	0.0055	2.143	0.034*	0.0009	0.0228

Significance levels: \*\*\*p-val.  $\leq 0.001$  (significant), \*\*p-val.  $\leq 0.01$  (very significant), \*p-val.  $\leq 0.05$  (highly significant).

Table 7: Multiple linear regression results for weight gain.

The second model is represented as

$$\begin{aligned} \text{WeightGain} = & 0.0003 \times \text{Time} - 1.2 \times 10^{-5} \times \text{Temp.} \times \text{Time} + \\ & + 0.0002 \times \text{Pr.Wat.} \times \text{Temp.} \times \text{Time} + 0.0049 \times \text{Pr.Wat.} \times \text{Time} + \\ & + 0.00017 \times \text{SeaWat.} \times \text{Temp.} \times \text{Time} + 0.0119 \times \text{SeaWat.} \times \text{Time} \end{aligned}$$

The simplified model equations are shown here



Machine oil: WeightGain =  $0.0003 \times \text{Time} - 1.2 \times 10^{-5} \times \text{Temp.} \times \text{Time}$

Pr. water: WeightGain =  $(0.0003 + 0.0049) \times \text{Time} + (-1.2 \times 10^{-5} + 0.0002) \times \text{Temp.} \times \text{Time}$

Sea water: WeightGain =  $(0.0003 + 0.0119) \times \text{Time} + (-1.2 \times 10^{-5} + 0.00017) \times \text{Temp.} \times \text{Time}$

These equations demonstrate that the slope of WeightGain vs Time is 0.0003 for machine oil,  $(0.0003 + 0.0049)$  for process water, and  $(0.0003 + 0.0119)$  for sea water respectively. There is a statistically significant effect only for sea water ( $t\text{-value} = 2.143$ ,  $p\text{-value} = 0.034$ ). Consequently, this suggests the weight gain increase of the material by 0.12 % for every 10 days inside the saline solution. Along with that, the interaction effect between temperature and time (WeightGain vs Temp.  $\times$  Time) is  $-1.2 \times 10^{-5}$  for oil,  $(-1.2 \times 10^{-5} + 0.0002)$  for process water, and  $(-1.2 \times 10^{-5} + 0.00017)$  for sea water respectively. Here, only 2 interactions are statistically significant for process ( $t\text{-value} = 2.461$ ,  $p\text{-value} = 0.015$ ) and sea water solutions ( $t\text{-value} = 2.180$ ,  $p\text{-value} = 0.031$ ). Accordingly, it indicates a 0.2 % and 0.17 % increase in weight gain of the material for process and sea water respectively for a 1000 unit increase in product 'Temp.  $\times$  Time'. In general, saline water affects weight gain stronger than process water. For instance, weight gain increases around 1.2 % and 1.0 % after 45 days at 90 °C inside sea and process water respectively.

As a result, it is apparent that weight gain can increase due to water and salt exposure. However, their effects on the interlaminar shear strength are different; the strength increases over time inside the sea water solution at room temperature, whereas it remains almost unchanged inside process water. It might be related to the additional reinforcement effect of the composite material because of salinity. Also, it may be a reason why process water promotes lower strength than the sea water relative to the control samples at high solution temperature. As we can see from Fig. 4, the maximum difference is around 4.7 MPa or 15 % and 3.8 MPa or 12 % after 45 days inside process and sea water respectively at 90 °C. The effect depends on the solution temperature: the higher temperature, the lower strength. Therefore, one can conclude that process water is more aggressive than sea water. On the contrary, the machine oil solution slightly affects the results: the maximum increase in strength is about 1.9 MPa or 6 %. This result needs further investigations because the significance level does not look high and there is a probability of about 3.2 % of obtaining that result by chance when the exposure time has no real effect. Moreover, there are no significant effects for weight gain results which also indicates the weak relationship between WeightGain vs Temp.  $\times$  Time.

## CONCLUSIONS

**S**eries of experimental studies of effects of preliminary hygrothermal aging at 22, 60 and 90 °C were conducted with the exposure time of 15, 30 and 45 days in aggressive operating media (sea water, process water, machine oil) for residual strength in case of interlaminar shear for specimens of STEF structural fiberglass. Characteristic loading diagrams and patterns of fiberglass specimen failure were obtained and analyzed before and after hygrothermal aging. It is observed that failure mechanisms change after hygrothermal aging in sea water and process water, which complies with the results of other authors in similar studies.

According to the ANCOVA analysis for multiple linear regression, increasing the exposure time of any solution studied does not have a statistically significant effect on the interlaminar shear strength and weight gain except for the sea water solution. It has a positive effect on strength values (about 1.25 MPa per 10 days rise in time) and weight gain (about 0.12 % per 10 days rise in time). Similarly, increasing the product of solution temperature and exposure time has a significantly positive effect on weight gain for process and sea water solutions. However, it has a significantly negative effect on the obtained strength values, but their effects are slightly different: process water is more aggressive than sea water. The biggest reduction of the interlaminar shear strength was observed at a temperature of 90 °C and a time of 45 days: around 12 % and 15 % for sea and process water solutions respectively. Probably, it might be associated with the additional reinforcement due to solution salinity. In addition, universal machine oil makes strength values slightly bigger. Similarly, this effect is dependant on solution temperature. For the specimens immersed in oil, the mean strength increases about 6 % after 45 days at 90 °C. Finally, the ANCOVA regression model has better predictive ability than the intercept-only one (predicts the average output for all the data) and can be successfully applied to predict the material strength after immersion tests into aggressive media.



## ACKNOWLEDGEMENTS

The work was carried out with support of the Russian Science Foundation (Project No. 21-79-10205, <https://rscf.ru/project/21-79-10205/>) in the Perm National Research Polytechnic University.

## REFERENCES

- [1] Lobanov, D.S., Wildemann, V.E., Spaskova, E. M., Chikhachev, A.I. (2015). Experimental investigation of the defects influence on the composites sandwich panels strength with use digital image correlation and infrared thermography methods. PNRPU Mechanics Bulletin, 4, pp. 159-170. DOI: 10.15593/perm.mech/2015.4.10
- [2] Lobanov, D.S., Babushkin, A.V. (2017). Experimental studies of the high temperature influence on strength and deformation properties of combined glass organoplastics. PNRPU Mechanics Bulletin, 1, pp. 104-117.
- [3] Lobanov, D.S., Slovikov, S.V. (2018). Mechanical behavior of a unidirectional basalt-fiber-reinforced plastic under thermomechanical loadings. Mechanics of Composite Materials, 54(3), pp. 351-358.
- [4] Lobanov, D.S., Babushkin, A.V., Luzenin, A.Yu. (2018). Effect of increased temperatures on the deformation and strength characteristics of a GFRP based on a fabric of volumetric weave. Mechanics of Composite Materials, 54(5), pp. 655-664.
- [5] de Souza, L.R., Marques, A.T., d'Almeida, J.R.M. (2017). Effects of aging on water and lubricating oil on the creep behavior of a GFRP matrix composite. Composite Structures, 168, pp. 285-291
- [6] Alam, P., Robert, C., Ó Brádaigh, C.M. (2018). Tidal turbine blade composites - A review on the effects of hygrothermal aging on the properties of CFRP. Composites Part B: Engineering, 149, pp. 248-259
- [7] Lobanov, D.S., Vildeman, V.E., Babin, A.D., Grinev, M.A. (2015). Experimental research into the effect of external actions and polluting environments on the serviceability of fiber-reinforced polymer composite materials. Mechanics of Composite Materials, 51(1), pp. 69-79
- [8] Muralidharan, M., Sathishkumar, T.P., Rajini, N., Navaneethakrishnan, P., Arun Kumar, S., Ismail, S.O., Senthilkumar, K., Siengchin, S. (2022). Evaluation of tensile strength retention and service life prediction of hydrothermal aged balanced orthotropic carbon/glass and Kevlar/glass fabric reinforced polymer hybrid composites, Journal of Applied Polymer Science, 139 (6), art. no. 51602. DOI: 10.1002/app.51602
- [9] Mansouri, L., Djebbar, A., Khatir, S., Abdel Wahab, M. (2019). Effect of hygrothermal aging in distilled and saline water on the mechanical behaviour of mixed short fibre/woven composites. Composite Structures, 207, pp. 816-825
- [10] Chen, Y., Davalos, J.F., Ray, I. (2006). Durability prediction for GFRP reinforcing bars using short-term data of accelerated aging tests. Journal of Composites for Construction, 10(4), pp. 279-286
- [11] Lobanov, D.S. Zubova, E.M. (2020). Temperature aging effects on mechanical behavior of structural GFRP on interlaminar shear tests. IOP Conf. Series: Materials Science and Engineering, 747.012119. DOI:10.1088/1757-899X/747/1/012119.
- [12] Park, S.Y., Choi, W.J., Choi, H.S. (2010). The effects of void contents on the long-term hygrothermal behaviors of glass/epoxy and GLARE laminates. Composite Structures, 92(1), pp. 18-24.
- [13] Malmstein, M., Chambers, A.R., Blake, J.I.R. (2013). Hygrothermal ageing of plant oil based marine composites Composite Structures, 101, pp. 138-143.
- [14] Li, Y., Li, R., Huang, L., Wang, K., Huang, X. (2016). Effect of hygrothermal aging on the damage characteristics of carbon woven fabric/epoxy laminates subjected to simulated lightning strike. Materials and Design, 99, pp. 477-489.
- [15] Lobanov, D.S., Lunegova, E.M., Mugatarov, A.I. (2021). Influence of preliminary thermal aging on the residual interlayer strength and staging of damage accumulation in structural carbon plastic. PNRPU Mechanics Bulletin, 1, pp.41-51. DOI: 10.15593/perm.mech/2021.1.05
- [16] Nicholas, J., Mohamed, M., Dhaliwal, G.S., Anandan, S., Chandrashekara, K. (2016). Effects of accelerated environmental aging on glass fiber reinforced thermoset polyurethane composites. Composites Part B: Engineering, 94, pp. 370-378.



- [17] Lu Z., Xian G., Li H. (2015). Effects of exposure to elevated temperatures and subsequent immersion in water or alkaline solution on the mechanical properties of pultruded BFRP plates. Composites Part B: Engineering, 77, pp. 421-430.
- [18] Lobanov, D. S., Zubova, E.M. (2019). Research of temperature aging effects on mechanical behaviour and properties of composite material by tensile tests with used system of registration acoustic emission signal. Procedia Structural Integrity, 18, pp. 347-352.
- [19] Amaro, A. M., Reis, P. N. B., Neto, M. A., & Louro, C. (2014). Effect of different commercial oils on mechanical properties of composite materials. Composite Structures, 118, 1–8. DOI:10.1016/j.compstruct.2014.07.017
- [20] Seltman H. J. Experimental Design and Analysis, (2018), 428 p.
- [21] Warner, R.M. (2013). Applied statistics : from bivariate through multivariate techniques.—2<sup>nd</sup>, 1691 p.
- [22] Elmushyakhi, A. (2021). Parametric characterization of nano-hybrid wood polymer composites using ANOVA and regression analysis. Structures, 29, pp. 652-662. DOI: 10.1016/j.istruc.2020.11.069
- [23] Bellini, C., Parodo, G., Polini, W., Sorrentino, L. (2018). Influence of hydrothermal ageing on single lap bonded CFRP joints, *Frattura ed Integrità Strutturale*, 45, pp.173-182.
- [24] Pehlivan, E., Roudnicka, M., Dzugan, J., Koukolikova, M., Kralik, V., Seifi, M., Lewandowski, J.J., Dalibor, D., Daniel, M. (2020). Effects of build orientation and sample geometry on the mechanical response of miniature CP-Ti Grade 2 strut samples manufactured by laser powder bed fusion. Additive Manufacturing, DOI: 10.1016/j.addma.2020.101403.
- [25] Alsahhaf, A., Spies, B. C., Vach, K., & Kohal, R.-J. (2017). Fracture resistance of zirconia-based implant abutments after artificial long-term aging. Journal of the Mechanical Behavior of Biomedical Materials, 66, pp. 224–232. DOI: 10.1016/j.jmbbm.2016.11.018.
- [26] Alamoush, R. A., Sung, R., Satterthwaite, J. D., Silikas, N. (2021). The effect of different storage media on the monomer elution and hardness of CAD/CAM composite blocks. Dental Materials. 37(7), pp. 1202-1213. DOI: 10.1016/j.dental.2021.04.009.
- [27] Durga Vithal, N., Bala Krishna, B., Gopi Krishna, M. (2021). Impact of dry sliding wear parameters on the wear rate of A7075 based composites reinforced with ZrB<sub>2</sub> particulates. Journal of Materials Research and Technology, 14, pp 174-185, DOI: 10.1016/j.jmrt.2021.06.005.
- [28] Osmond, R., Mollahoseini, Z., Singh, J., Gautam, A., Seethaler, R., Golovin, K., Milani, A. S. (2021). A group multicriteria decision making with ANOVA to select optimum parameters of drilling flax fibre composites. Composites Part C, 5, 100156, DOI: 10.1016/j.jcomc.2021.100156.
- [29] Balachandhar, R., Balasundaram, R., Ravichandran, M. (2021). Analysis of surface roughness of rock dust reinforced AA6061-Mg matrix composite in turning. Journal of Magnesium and Alloys, DOI: 10.1016/j.jma.2021.03.035.
- [30] Karthik, A., Srinivasan, S.A., Karunanithi, R., Kumares Babu, S.P., Kumar, V., Jain, S. (2021). Influence of CeO<sub>2</sub> reinforcement on microstructure, mechanical and wear behaviour of AA2219 squeeze cast composites. Journal of Materials Research and Technology, 14, pp. 797-807, DOI: 10.1016/j.jmrt.2021.06.056.
- [31] Kim, N. K., Bruna, F.G., Das, O., Hedenqvist, M. S., Bhattacharyya, D. (2020). Fire-retardancy and mechanical performance of protein-based natural fibre-biopolymer composites. Composites Part C, 1, 100011, DOI : 10.1016/j.jcomc.2020.100011.
- [32] Reis, P.N.B., Silva, A.P., Santos, P., Ferreira, J.A.M. (2013). Hygrothermal effect on the impact response of carbon composites with epoxy resin enhanced by nanoclays. Mech Compos Mater, 49, pp.429–436.
- [33] Boukhounda, B.F., Adda-Bedia, E., Madani, K. (2006). The effect of fiber orientation angle in composite materials on moisture absorption and material degradation after hygrothermal ageing. Compos Struct; 74, pp.406–418.